Australian Earthquake Engineering Society
National Conference, 21-23 November 2024
Adelaide, South Australia

Evaluation of the NSHA23 Magnitude Conversion Equations Using a New Moment Magnitude Catalogue

Trevor I Allen[1]

1. Geoscience Australia, Symonston ACT 2609

Abstract

An earthquake catalogue based on the moment magnitude scale (M_W) is a prerequisite for global best practice seismic hazard analyses. The 2018 National Seismic Hazard Assessment (NSHA18) was the first national-scale seismic hazard assessment for Australia to apply magnitude conversions to express earthquake magnitudes uniformly in terms of M_W. This approach led to the single-biggest change in seismic hazard estimates between Geoscience Australia-led national seismic-hazard models. Between the 2012 and 2018 assessments, the hazard reduced because of: 1) the general reduction in the number of earthquakes of magnitude 4.0 and larger due to the correction of local magnitudes (M_L) and subsequent conversion to M_W, and; 2) the increase in the Gutenberg-Richter *b*-value due to the non-linear conversion of local magnitudes M_L to M_W.

Using a new continental-scale attenuation model, independent assessment of M_W has been performed for over 300 earthquakes recorded between 1990 and September 2024. After recalculating M_L for the same earthquakes using improved filtering and time-domain windowing criteria, the M_W catalogue is used to test and validate the M_L to M_W conversion equations used in the 2023 National Seismic Hazard Assessment (NSHA23). The earthquakes are partitioned into their regional magnitude polygons as applied by Geoscience Australia in its real-time operations; notionally central and western Australia, South Australia (Mt Lofty and Flinders Ranges) and eastern Australia. The performance of the NSHA23 M_L to M_W conversion equation is then assessed for each of these magnitude regions. Overall, the NSHA23 M_L to M_W conversion performs very well relative to the continental-scale earthquake dataset. The sensitivity of this conversion to an earthquake's static stress drop is also assessed. There is evidence that minor adjustments could be applied to the NSHA23 M_L–M_W conversion equation for larger-magnitude events with high stress drops.

Keywords: NSHA23, magnitude conversion equations, local magnitude, moment magnitude.

1 Introduction

The key components of probabilistic seismic-hazard assessments (PSHAs) are an accurate representation of earthquake sources to determine the rupture forecast model and a ground-motion characterisation model. In modern-day PSHAs, the magnitude type applied is almost universally represented by the moment magnitude scale (M_W). This is largely because there is a requirement for self-consistency between the magnitude type used to derive the rupture forecast model (or earthquake rate model), and the magnitude type to which all modern ground-motion models (GMMs) are calibrated (e.g., International Atomic Energy Agency, 2022).

The use of an earthquake catalogue uniformly expressed in terms of M_W was first suggested for national seismic-hazard assessments in Australia by Allen *et al.* (2011) for the 2012 National Seismic Hazard Map project (NSHM12; Burbidge, 2012). Allen *et al.* (2011) proposed the use of two independent conversion equations; one for eastern Australia and another for central and western Australia. However, this catalogue harmonisation approach was ultimately discarded because of concerns that the magnitude conversions yielded *b*-values that were considered unrealistic at the time (Leonard *et al.*, 2014). The 2018 National Seismic Hazard Assessment (NSHA18) was the first national-scale assessment to use a homogenised earthquake catalogue to underpin the earthquake rate model (Allen *et al.*, 2018; 2020). This change led to the single-largest difference in hazard relative to the 2012 model (e.g., Griffin *et al.*, 2020). These conversions were updated for the 2023 National Seismic Hazard Assessment (NSHA23) due to improved knowledge in the calibration coefficients used in Australian seismological observatories for the Wood-Anderson torsion seismometer (Anderson and Wood, 1925), which is required to calculate M_L (Allen *et al.*, 2023). Due to the relative abundance of local magnitude estimates in the Australian earthquake catalogue, the most important magnitude conversion is that between M_L and M_W. In addition to the M_L–M_W conversion, additional conversions have been developed for different magnitude types. In particular, these include body-wave magnitude (m_b), and surface-wave magnitude (M_S).

This paper explores the development of the NSHA23 magnitude conversion equations from M_L and m_b and evaluates their performance relative to new improved source parameters for Australian earthquakes (Allen, 2024; in prep); in particular, M_W.

2 NSHA23 Catalogue Homogenisation

The NSHA23 updated magnitude conversion equations developed through the NSHA18 based on new data, and updated knowledge on Australian observational practice. These new conversions use orthogonal-distance regression (e.g., Castellaro *et al.*, 2006) between M_L, m_b and M_S and M_W (Allen *et al.*, 2024; in prep). Below, the approach to updating the M_L–M_W and m_b–M_W conversions for use in the NSHA23 is discussed.

2.1 Local Magnitude

In revising the M_L–M_W conversion for the NSHA23, adjustments were made to the calibration of Wood-Anderson displacement amplitudes (e.g., Uhrhammer and Collins, 1990) to ensure improved consistency with legacy catalogue magnitudes. To update the conversion, simulated time-histories are used to approximate the relativity between the two magnitude types. This approach is detailed in Appendix B of Allen *et al.* (2023).

In summary, time-histories for given magnitude-distance couples were simulated using the SMSIM software (Boore, 2002, 2003) using Fourier attenuation coefficients of Allen *et al.* (2007) for southeastern Australia. Simulated data were generated for a total of 500 earthquakes sampled randomly with magnitudes $2.0 \leq M_W \leq 6.5$. For each event in this

simulated M_W catalogue, the number of stations that would have recorded that event assuming typical station distribution for southeastern Australia was sampled (Allen *et al.*, 2023). Using the number of sampled stations, the station hypocentral distances (R_{hyp}) were subsequently randomly sampled.

Simulated vertical-component acceleration time-histories were then converted to Wood-Anderson displacement time histories and the peak trace amplitude was extracted for the calculation of local magnitude. Each synthetic seismogram assumes a damping (h) = 0.8, natural frequency (f_0) of 1.25 Hz and a static magnification of 2,800 (Richter, 1935). For each simulated earthquake with a 'known' M_W, the mean M_L from all of the simulated stations was determined using the eastern Australian M_L relationship of Michael-Leiba and Malafant (1992), including the vertical-to-horizontal-component correction of 0.13 magnitude units. These simulated M_W and M_L data were then fitted using a quadratic functional form. The coefficients for this regression are provided in Allen *et al.* (2023).

One limitation in this simulated relationship is that it only uses Fourier attenuation coefficients and the M_L relationship for eastern Australia. Thus, there is an inherent assumption that the relativity between M_L and M_W will be same for all Australian regions.

2.2 Body-wave Magnitude

A list of earthquakes with event-specific body-wave magnitude m_b and M_W was compiled from the NSHA23 earthquake catalogue. Through the NSHA23 analyses, existing m_b to M_W conversion equations developed for other global regions were assessed. It was found that existing conversion equations were highly variable and not appropriate for the Australian earthquake catalogue (e.g., Allen *et al.*, 2018). Body-wave magnitude for those earthquakes that also possess a M_W value within continental Australia were extracted from the earthquake catalogue for earthquakes of magnitude $3.5 \leq m_b \leq 6.0$. For the NSHA23, a bi-linear relationship between m_b and M_W was found to be the most appropriate model for the Australian earthquake catalogue. The coefficients for this regression are also provided in Allen *et al.* (2023).

3 Testing NSHA23 Magnitude Conversions with New Data

A new study by Allen (2024; in prep) has undertaken an independent assessment of M_W for over 300 earthquakes recorded between 1990 and September 2024. These moment magnitudes are resolved from fitting the source-corrected displacement Fourier spectrum assuming the ω^{-2} source model (Brune, 1970). In the present section, the approach to reviewing the NSHA23 M_L–M_W and m_b–M_W conversions are discussed in more detail.

3.1 Local Magnitude

For each of the earthquakes in the Allen (2024; in prep) dataset, local magnitudes have been calculated applying the approaches recommended by the NSHA23 (Allen *et al.*, 2023), with the exception that *Rg* phases, which are common for shallow-focus earthquakes, are also not considered when picking the peak Wood-Anderson displacement amplitudes. This improvement in approach means that only body waves are considered for the calculation of the earthquake magnitudes.

Figure 1 shows the new moment magnitude calculations relative to updated local magnitudes (Allen, 2024; in prep). This figure shows that there is generally excellent correspondence between the new empirical data and the NSHA23 M_L–M_W conversion equation based on simulated data. The new data are also regressed to determine whether there are significant differences between the new data and the proposed regression in the NSHA23. Whilst there are some minor differences, the NSHA23 regression is currently preferred given that the

simulations sample the full magnitude range uniformly. However, it is observed that larger earthquakes appear to have relatively larger M_L in comparison to M_W and the NSHA23 conversion does not accurately reflect this. This said, these earthquakes are rare in the catalogue and have limited effect on regional-scale earthquake recurrence rates. Furthermore, these earthquakes also usually have independent estimates of M_W and thus a conversion is not generally required for modern events. Nevertheless, these higher stress-drop earthquakes at larger magnitudes will have consequences for ground-motion forecasts, and are thus, are an important consideration in ground-motion model selection.

Figure 2 shows the residuals of new moment magnitude estimates relative to moment magnitudes estimated using the NSHA23 M_L–M_W conversion equations with the M_L estimates from Allen (2024; in prep). The figure shows the residuals for: all data (Figure 2a); eastern Australia, which applies the Michael-Leiba and Malafant (1992) M_L algorithm (Figure 2b); central and western Australia, which applies the Gaull and Gregson (1991) M_L algorithm (Figure 2c), and; south Australia, which applies the (Greenhalgh and Singh, 1986) M_L algorithm (Figure 2d). Whilst there is clearly some scatter in those residuals, the mean residual for all regions is close to zero. Furthermore, while not explicitly considered in this paper, there is a clear dependence in the M_W residuals with the Brune (1970) stress-drop parameter. What these residuals show is that higher stress-drop earthquakes will have relatively higher estimates of M_L, while lower stress-drop earthquakes will have relatively higher estimates of M_W. An observation for the larger-magnitude earthquakes is that they tend to have high stress drops. This observation is particularly apparent for the western and central Australia region where the larger events appear to have a larger misfit relative to the NSHA23 conversion (Figure 2c). It is also worth noting that the NSHA23 conversion assumes only the Michael-Leiba and Malafant (1992) M_L algorithm for eastern Australia, and as such, there may be some biases relative to the western and central, and south Australian datasets due to different attenuation characterisation conditions of each dataset. However, the larger source of bias is more likely to stem form the higher stress drop for these data.

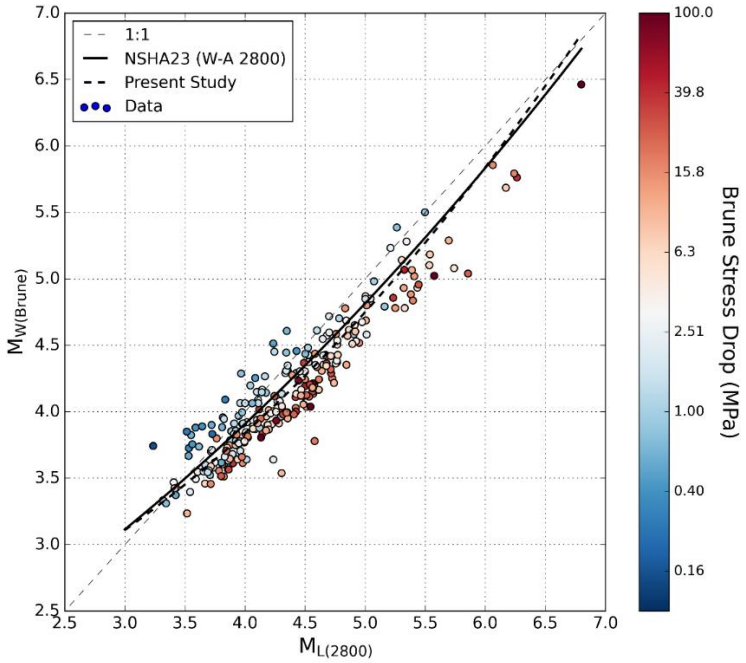

Figure 1. New moment magnitude calculations relative to updated local magnitudes (Allen, 2024; in prep). Datapoints are color-coded by Brune stress drop (Δσ) estimates. The NSHA23 M_L-M_W conversion is shown as the thick black line. The regression between the empirical M_L and M_W data is shown with the thick dashed line.

3.2 Body-wave Magnitude

Unlike the analysis for M_L in the previous section, body-wave magnitudes, m_b, are taken directly from the Geoscience Australia online catalogue for the post-1990 events analysed.

The m_b–M_W couples for the post-1990 events were augmented with pre-1990 events with both m_b and M_W estimates from the NSHA23 catalogue. Figure 3 shows this combined dataset of m_b and M_W data relative to the NSHA23 m_b–M_W bi-linear relationship. This updated dataset, again shows remarkably good correspondence with the NSHA23 relationship. Fitting the data with a linear relationship for small-magnitude earthquakes, transitioning into a quadratic relationship for larger magnitudes yields a similarly shaped function to bi-linear relationship developed for the NSHA23. However, the new relationship—which uses orthogonal-distance regression—yields lower estimates of M_W for a given m_b. Given this is a more complete dataset than that used for the NSHA23, the coefficients for this revised relationship are preferred. The functional form is:

$$M_W = a \times m_b + b \text{ for } m_b \leq M_{hx} \quad (1a)$$

$$M_W = c \times (m_b - M_{hx}) + d \times (m_b - M_{hx})^2 + M_{hy} \text{ for } m_b > M_{hx} \quad (1b)$$

where a = 1.083, b = -0.7917, c = 1.966, d = -0.1058, M_{hx} = 5.656, and:

$$M_{hy} = a \times M_{hx} + b \quad (1c)$$

The standard deviation for this revised relationship is 0.17 magnitude units.

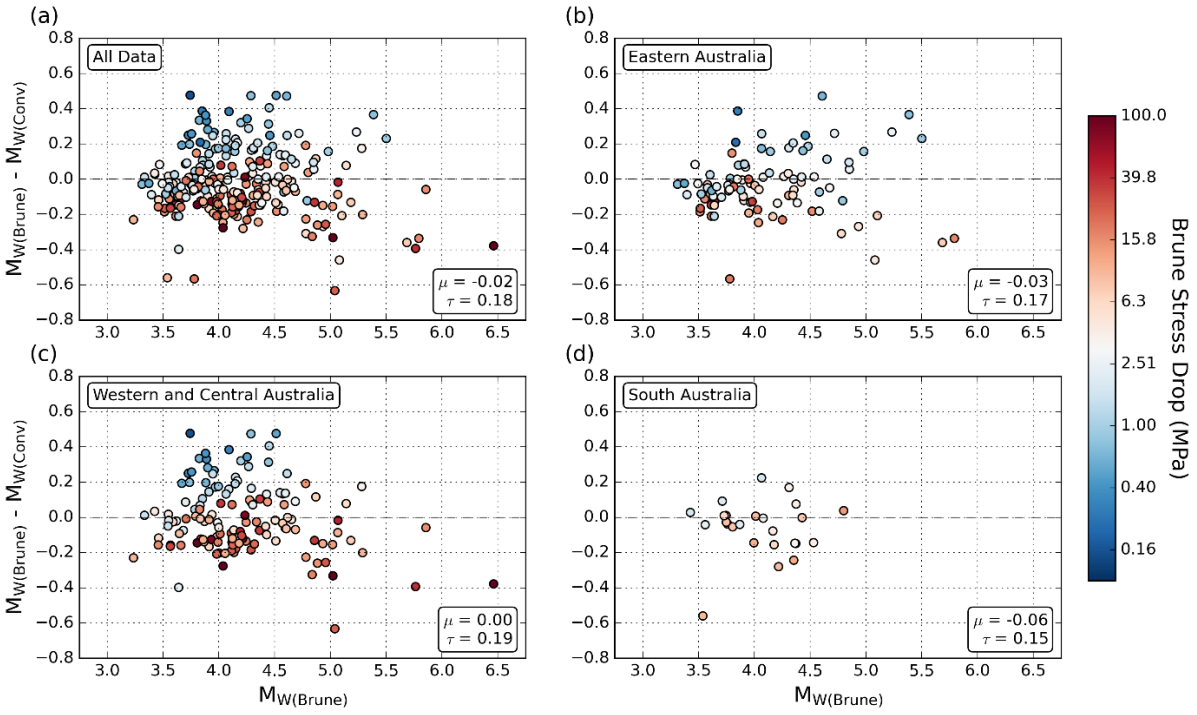

Figure 2. Residual of new moment magnitude estimates ($M_{W(Brune)}$) relative to the NSHA23 M_L-M_W conversion ($M_{W(Conv)}$). The data are color-coded relative to the estimated stress drop ($\Delta\sigma$). Residuals are shown for (a) all data; (b) the eastern Australian region; (c) the western and central Australian region, and; (d) the South Australian region. The mean (μ) and standard deviation (τ) of the residuals are shown for each subplot.

4 Discussion and Conclusion

The use of magnitude conversion equations for catalogue homogenisation for the NSHA18 change led to the single-largest difference in hazard relative to the 2012 model (e.g., Griffin *et al.*, 2020). Alternative methods to explore the application of conversion equations in the PSHA workflow have been explored previously (Ghasemi and Allen, 2017). As described in the current contribution, the number of earthquakes with independent estimates of local and

moment magnitudes are limited within the Australian catalogue. As more data become available, magnitude conversions will converge on a more stable conversion relationship. These conversions are not only sensitive to the moment magnitude estimates, but also to the assumptions used in the estimation of M_L. Thus, the overall seismic hazard forecasts are sensitive to these relationships. Nevertheless, the NSHA23 relationships are, in general, consistent with empirical and theoretical observations from the international hazard modelling community (e.g., Hanks and Boore, 1984; Edwards *et al.*, 2010; 2015; Munafò *et al.*, 2016; Deichmann, 2017; Dost *et al.*, 2018; Staudenmaier *et al.*, 2018).

This paper explores the performance of the NSHA23 equations that convert local magnitudes, M_L, and body-wave magnitudes, m_b, to M_W using a new M_W dataset of over 300 earthquakes (Allen, 2024; in prep). In general, both of the NSHA23 conversions tested perform very well relative to the new dataset. The NSHA23 M_L–M_W conversion equation performs particularly well for small-magnitude earthquakes. This is important because it is these events that have a larger impact on the Gutenberg and Richter (1944) magnitude-frequency distributions used in the seismic source characterisation of the NSHA23. However, there may be a need to adjust this conversion for larger-magnitude events, which appear to have higher Brune (1970) stress drops and larger residuals relative to the mean estimate from the conversion.

The NSHA23 m_b–M_W conversion also performs remarkably well relative to the newly compiled dataset from Allen (2024; in prep) for post-1990 earthquakes and from Allen *et al.* (2018) for pre-1990 earthquakes. Fitting these new data yields a conversion similar to the NSHA23 m_b–M_W conversion, but removes a small, but systematic bias (Figure 3).

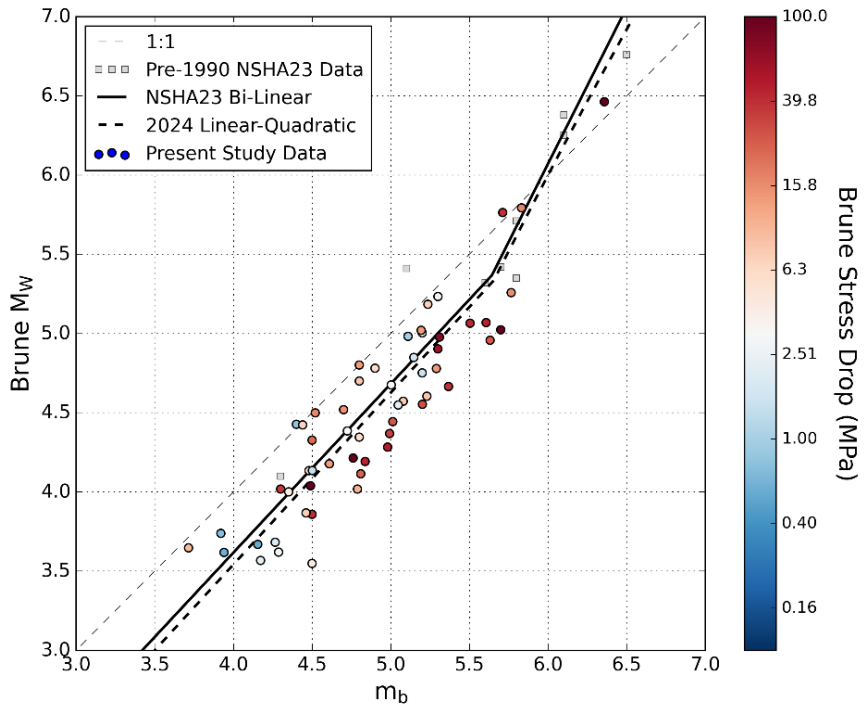

Figure 3. Relationships between calculated moment magnitudes M_W for Australian earthquakes versus the preferred local magnitudes m_b. The thick dashed line shows the linear least-squares fit to the post-1990 data, while the solid bi-linear line shows the relationship developed for the NSHA23. The thin dashed line represents a 1:1 relationship with m_b.

Using a new, independent dataset of earthquake magnitude estimates has verified the utility of the use of the NSHA23 magnitude conversion equations for use in homogenising Australian earthquake catalogues for use in seismic hazard assessments. These data have demonstrated

a clear trend in the residuals when using the NSHA23 M_L–M_W conversion, with earthquakes having high stress drops having relatively higher values of M_L, and with low stress-drop events having relatively higher values of M_W. Larger-magnitude events also appear to possess systematically larger stress drops and may suggest that the NSHA23 M_L–M_W conversion may require a stress-drop adjustment based on the predominant magnitude. However, in the modern era, larger-magnitude earthquakes will likely already have preferred magnitudes of M_W and thus will not require conversion. Nevertheless, these higher stress-drop earthquakes at larger magnitudes will have consequences for ground-motion forecasts, and are thus, are an important consideration in ground-motion model selection.

5 References

Allen, T. I. (2024; in prep). Systematic estimation of earthquake source parameters for continental Australia, *Bull. Seismol. Soc. Am.*

Allen, T. I., D. R. Burbidge, D. Clark, A. A. McPherson, C. D. N. Collins, and M. Leonard (2011). Development of the next generation Australian National Earthquake Hazard Map, *Ninth Pacific Conference on Earthquake Engineering*, Auckland, New Zealand.

Allen, T. I., P. R. Cummins, M. Çomoğlu, S. S. Martin, and W. Peck (2024; in prep). The 2023 National Seismic Hazard Assessment for Australia: earthquake hypocentre catalogue, *Geoscience Australia Record 2024/XX*, doi: 10.26186/149186.

Allen, T. I., P. R. Cummins, T. Dhu, and J. F. Schneider (2007). Attenuation of ground-motion spectral amplitudes in southeastern Australia, *Bull. Seismol. Soc. Am.* **97,** 1279–1292, doi: 10.1785/0120060172.

Allen, T. I., J. D. Griffin, D. J. Clark, P. R. Cummins, H. Ghasemi, and R. Ebrahimi (2023). The 2023 National Seismic Hazard Assessment for Australia: model overview, *Geoscience Australia Record 2023/53*, 152 pp, doi: 10.26186/148969.

Allen, T. I., J. D. Griffin, M. Leonard, D. J. Clark, and H. Ghasemi (2020). The 2018 National Seismic Hazard Assessment of Australia: quantifying hazard changes and model uncertainties, *Earthq. Spectra* **36,** 5-43, doi: 10.1177/8755293019900777.

Allen, T. I., M. Leonard, H. Ghasemi, and G. Gibson (2018). The 2018 National Seismic Hazard Assessment for Australia: earthquake epicentre catalogue, *Geoscience Australia Record 2018/30*, Canberra, 51 pp, doi: 10.11636/Record.2018.030.

Anderson, J. A., and H. O. Wood (1925). Description and theory of the torsion seismometer, *Bull. Seismol. Soc. Am.* **15,** 1-72, doi: 10.1785/BSSA0150010001.

Boore, D. M. (2002). SMSIM — Fortran programs for simulating ground motions from earthquakes: Version 2.0 — a revision of OFR 96–80–A, *U.S. Geological Survey Open-File Report 00 – 509*, Menlo Park, California, 56 pp.

Boore, D. M. (2003). Simulation of ground motion using the stochastic method, *Pure appl. geophys.* **160,** 635-676, doi: 10.1007/PL00012553.

Brune, J. N. (1970). Tectonic stress and the spectra of seismic shear waves from earthquakes, *J. Geophys. Res.* **75,** 4997-5009, doi: 10.1029/JB075i026p04997.

Burbidge, D. R., Ed. (2012). *The 2012 Australian Earthquake Hazard Map*, Geoscience Australia Record 2012/71.

Castellaro, S., F. Mulargia, and Y. Y. Kagan (2006). Regression problems for magnitudes, *Geophys. J. Int.* **165,** 913–930, doi: 10.1111/j.1365-246X.2006.02955.x.

Deichmann, N. (2017). Theoretical basis for the observed break in M_L/M_W scaling between small and large earthquakes, *Bull. Seism. Soc. Am.* **107,** 505-520, doi: 10.1785/0120160318.

Dost, B., B. Edwards, and J. J. Bommer (2018). The relationship between **M** and M_L: a review and application to induced seismicity in the Groningen Gas Field, The Netherlands, *Seism. Res. Lett.* **89,** 1062-1074, doi: 10.1785/02201700247.

Edwards, B., B. Allmann, D. Fäh, and J. Clinton (2010). Automatic computation of moment magnitudes for small earthquakes and the scaling of local to moment magnitude, *Geophys. J. Int.* **183,** 407–420, doi: 10.1111/j.1365-246X.2010.04743.x.

Edwards, B., T. Kraft, C. Cauzzi, P. Kästli, and S. Wiemer (2015). Seismic monitoring and analysis of deep geothermal projects in St Gallen and Basel, Switzerland, *Geophys. J. Int.* **201,** 1022–1039, doi: 10.1093/gji/ggv059.

Gaull, B. A., and P. J. Gregson (1991). A new local magnitude scale for Western Australian earthquakes, *Aust. J. Earth. Sci.* **38,** 251-260, doi: 10.1080/08120099108727970.

Ghasemi, H., and T. Allen (2017). Testing the sensitivity of new Australian empirical magnitude conversion equations on seismic hazard analyses, *Australian Earthquake Engineering Society 2017 Conference*, Canberra, ACT.

Greenhalgh, S. A., and R. Singh (1986). A revised magnitude scale for South Australian earthquakes, *Bull. Seismol. Soc. Am.* **76,** 757-769, doi: 10.1785/BSSA0760030757.

Griffin, J. D., T. I. Allen, and M. C. Gerstenberger (2020). Seismic hazard assessment in Australia: can structured expert elicitation achieve consensus in the "land of the fair go"?, *Seismol. Res. Lett.* **91,** 859–873, doi: 10.1785/0220190186.

Gutenberg, B., and C. F. Richter (1944). Frequency of earthquakes in California, *Bull. Seismol. Soc. Am.* **34,** 185-188, doi: 10.1785/BSSA0340040185.

Hanks, T. C., and D. M. Boore (1984). Moment-magnitude relations in theory and practice, *J. Geophys. Res.* **89,** 6229-6235, doi: 10.1029/JB089iB07p06229.

International Atomic Energy Agency (2022). Seismic hazards in site evaluation for nuclear installations: safety guide, *International Atomic Energy Agency Specific Safety Guide No. SSG-9 (Rev. 1)*, Vienna, 78 pp.

Leonard, M., D. R. Burbidge, T. I. Allen, D. J. Robinson, A. McPherson, D. Clark, and C. D. N. Collins (2014). The challenges of probabilistic seismic-hazard assessment in stable continental interiors: an Australian example, *Bull. Seismol. Soc. Am.* **104,** 3008-3028, doi: 10.1785/0120130248.

Michael-Leiba, M., and K. Malafant (1992). A new local magnitude scale for southeastern Australia, *BMR J. Aust. Geol. Geophys.* **13,** 201-205.

Munafò, I., L. Malagnini, and L. Chiaraluce (2016). On the relationship between M_W and M_L for small earthquakes, *Bull. Seism. Soc. Am.* **106,** 2402-2408, doi: 10.1785/0120160130.

Richter, C. F. (1935). An instrumental earthquake magnitude scale, *Bull. Seismol. Soc. Am.* **25,** 1-32, doi: 10.1785/BSSA0250010001.

Staudenmaier, N., T. Tormann, B. Edwards, N. Deichmann, and S. Wiemer (2018). Bilinearity in the Gutenberg-Richter relation based on M_L for magnitudes above and below 2, from systematic magnitude assessments in Parkfield (California), *Geophys. Res. Lett.* **45,** 6887-6897, doi: 10.1029/2018GL078316.

Uhrhammer, R. A., and E. R. Collins (1990). Synthesis of Wood-Anderson seismograms from broadband digital records, *Bull. Seismol. Soc. Am.* **80,** 702-716, doi: 10.1785/BSSA0800030702.